The Effect of a Finite Measurement Volume on Power Spectra from a Burst Type LDA

Buchhave, Preben; Velte, Clara Marika; K. George , William

Published in:
Proceedings of the 17th International Symposium on Applications of Laser Techniques to Fluid Mechanics

Publication date:
2014

Document Version
Peer reviewed version

The Effect of a Finite Measurement Volume on Power Spectra from a Burst Type LDA

Preben Buchhave[1,*], Clara M. Velte[2], and William K. George[3]

1. Intarsia Optics, Birkerød, Denmark
2. Technical University of Denmark, Lyngby, Denmark
3. Princeton University, Princeton, NJ, USA
* correspondent author: preben.buchhave@gmail.com

Abstract. We analyze the effects of a finite size measurement volume on the power spectrum computed from data acquired with a burst-type laser Doppler anemometer. The finite measurement volume causes temporal distortions in acquisition of the data resulting in phenomena such as finite processing time and dead time. We compare analytical expressions for the bias and distortion of the velocity power spectrum computed from computer-generated data. We then compare the spectrum from the computer-generated data and a power spectrum from a measurement on a free turbulent jet in air and conclude that we have a valid understanding of the effects of the finite measurement volume on the measured velocity power spectrum.

1. Introduction

Power spectral estimation of a random process such as a turbulent velocity has been the subject of intense investigation (Gaster *et al.* 1975, Gaster *et al.* 1977, Buchhave *et al.* 1979), and it is recognized that the finite size of the measurement volume limits the spatial and temporal resolution of the sampled velocity. However, during our experimental work we noticed an unexpected distortion and bias of the computed velocity power spectrum in the form of a dip in the high frequency part and a distortion of the overall shape at lower frequencies (Velte *et al.* 2014). Similar effects have been described in photo counting (Zhang *et al.* 1995), and dead time effects we anticipated in early LDA burst type LDA measurements, but due to the limited computer facilities the problem was not analyzed in detail (Gaster 2013).
As we shall demonstrate in this paper, we attribute these problems to the fact that a burst-type LDA data point is obtained from a finite length digitized velocity trace sampled within the measurement volume, and that a subsequent data point cannot be obtained until the current measurement is concluded. The fact that the sampling process is thus not an idealized point sampling in space and time has a profound influence on the measured power spectrum.
In the following, we illustrate the effects of the finite sampling time and the finite dead time on a power spectrum computed from data obtained with a burst-type LDA.

2. Sampling

Figure 1 illustrates a typical LDA burst. The Gaussian curve (red) represents the envelope of the Doppler modulated signal burst from the photo detector. We assume a burst detection circuit that allows deciding when the envelope exceeds a certain threshold voltage, the trigger level. The period of time in which the signal envelope is above the trigger level we call the residence time (or transit time) Δt_s. It is basically the time a seed particle spends in the measurement volume. However, most signal processors sample the signal for a finite time after the initial burst detection and perform frequency detection by a fixed length FFT. This time we call the processing time, Δt_p. Even after completing the frequency detection, the processor will be inactive and unable to receive a subsequent Doppler burst until the present envelope has decreased below the trigger level, and the current measurement has been sent off to the data processor. The period in which the signal processor is unable to receive a subsequent burst we denote the dead time, Δt_d.

In the following we distinguish between the process to be measured, the "true velocity", $u(t)=u'(t)+\bar{u}$, where $u'(t)$ is the fluctuating part and $\bar{u}$ is the mean velocity, and the measured velocity, $u_0(t)=u_0'(t)+\bar{u}_0$. By the "signal" we understand the electronic signal presented to the signal processor.

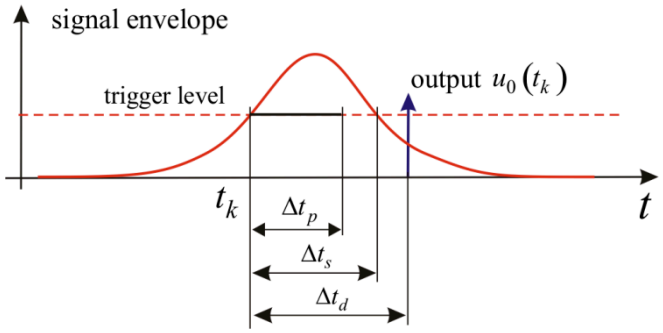

Fig 1. LDA burst illustrating arrival time, t_k, processing time, Δt_p, residence time, Δt_s, and dead time, Δt_d.

In Buchhave *et al.* (2014) we analyzed the effects of a finite processing time, a finite residence time and a finite dead time on the shape of the power spectrum computed from a record of randomly arriving data of record length T, arriving at a mean data rate ν. We shall not repeat the derivations here, but just summarize the results.

The effect of the finite processing time Δt_p is that the velocity fluctuations are smoothed out and averaged during that period. In essence, the processing time represents a rectangular time window. After the FFT process, this time window is converted to a sinc-squared frequency window, a transmission function multiplying the true velocity spectrum, $S_u(f)$:

$$S_{u,\Delta t_p}(f)=S_u(f)\cdot \mathrm{sinc}^2(\pi f \Delta t_p) \qquad (1)$$

$S_{u,\Delta t_p}(f)$ represents the quantity measured by the processor.

3. Dead time

The fact that the processor is disabled during the dead time further modifies the measured data. The term non-paralyzable dead time means that the processor is totally insensitive to new data arriving within the dead time. Paralyzable dead time refers to a situation where a processor restarts or continues a measurement even if new data arrive within the dead time. If the data rate is high enough this may result in a situation where the processor is stuck with the first sample and is unable to provide more data; the processor is paralyzed.

Fixed non-paralyzable dead time

In the time domain, the presence of Δt_d means that the time lag between measured data cannot be smaller than Δt_d. In case of a fixed dead time this would simply mean a lack of data with time-between-samples smaller than Δt_d, and it would be visible in the sampled autocovariance function (ACF) as a void of samples between time zero and plus and minus Δt_d. The ACF resulting from the dead time effect can be represented as the product of the ACF computed from the filtered velocity, $C_{u,\Delta t_p}(\tau)$, and a function $\left(1-\Pi_{2\Delta t_d}(\tau)\right)$ removing all lags τ in the range $-\Delta t_d<\tau<\Delta t_d$:

$$C_{0,\Delta t_p,\Delta t_d}(\tau) = C_{u,\Delta t_p}(\tau)\cdot\left(1-\Pi_{2\Delta t_d}(\tau)\right) \qquad (2)$$

where $\Pi_{2\Delta t_d}(\tau)$ is a top hat function equal to one between +- Δt_d. The ACF resulting from a fixed dead time is shown in Figure 2:

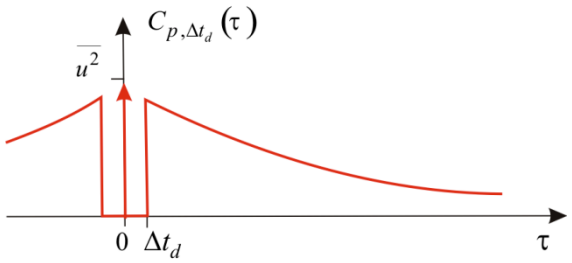

Fig 2. Autocovariance function with dead time effect.

Because of the data lost during the dead time, the data rate is reduced: $\nu_0 = \nu e^{-\nu\Delta t_d}$ (Buchhave *et al.* 2014) .

The effect on the spectrum is a convolution between the filtered spectrum and a dead time frequency function:

$$S_{u,\Delta t_p,\Delta t_d}(f) = S_{u,\Delta t_p}(f)\otimes\left[\delta(f) - 2\Delta t_d\ \mathrm{sinc}\left(2\pi f\Delta t_d\right)\right] \qquad (3)$$

The quantity $S_{u,\Delta t_p,\Delta t_d}$ represents the power spectrum modified by the existence of a finite measurement volume through the finite processing time and the finite dead time. However, the final result of the measurement, $S_{0,u,\Delta t_p,\Delta t_d}(f)$, also depends on the algorithm for computation of the power spectrum used in the data processor. If, for example, we employ the so-called direct method, the spectrum is computed for individual blocks of data from the estimator given by:

$$S_0(f) = \frac{1}{T}\hat{u}(f)^*\,\hat{u}(f) \qquad (4)$$

where $\hat{u}(f)$ is the Fourier transform of the measured signal. If we do not exclude self-products in the computation, the computed spectrum will include a constant term of the same magnitude at all frequencies, a quantity we call the spectral offset:

$$S_{0,\Delta t_p,\Delta t_d}(f) = \frac{\overline{u^2_{\Delta t_p,\Delta t_d}}}{\nu_0} + \left[S_{u,\Delta t_p}(f)\otimes\left[\delta(f) - 2\Delta t_d\ \mathrm{sinc}\left(2\pi f\Delta t_d\right)\right]\right] \qquad (5)$$

$$= \frac{\overline{u^2_{\Delta t_p,\Delta t_d}}}{\nu_0} + \left[\left(S_u(f)\cdot\mathrm{sinc}^2\left(\pi f\Delta t_p\right)\right)\otimes\left[\delta(f) - 2\Delta t_d\ \mathrm{sinc}\left(2\pi f\Delta t_d\right)\right]\right] \qquad (6)$$

The first term is the spectral offset described above. The second term is the convolution of the filtered spectrum with the dead time function. We may of course attempt to subtract the spectral offset along with other white noise terms to obtain a greater dynamic range in the plot.

If both Δt_p and Δt_d go to zero (infinitely small measuring volume, delta-function sampling), we get the conventional averaged result

$$S_0(f) = \frac{\overline{u^2}}{\nu} + S_u(f) \tag{7}$$

where the first term is the spectral offset and the second one is the desired spectrum. In Figure 3 we illustrate the effects of sample frequency and dead time. $\Delta t_p = \Delta t_d = 0.00002$ corresponds to the average mean time between samples if sampled at approximately the Nyquist rate. The spectra include the offset caused by the self-product terms.

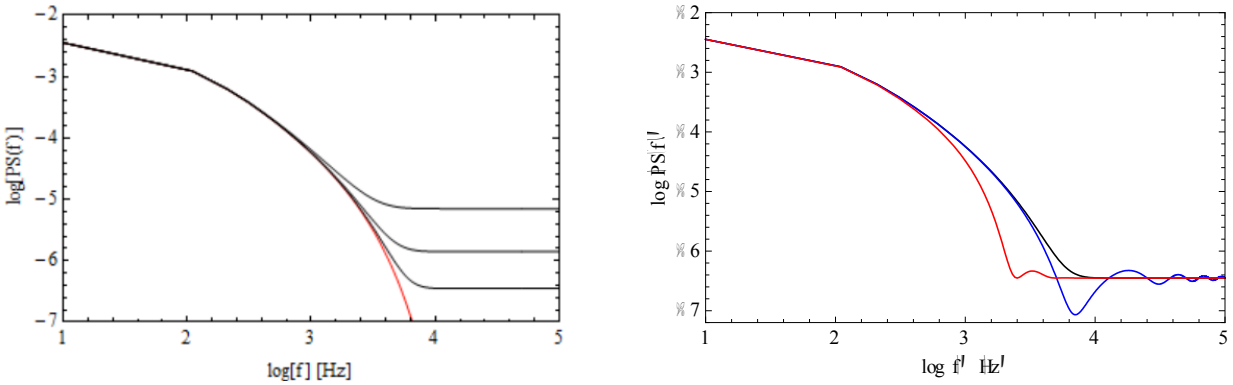

Fig 3. The effect of dead time on a Von Karman power spectrum.
Left: Red: Model von Karman spectrum. Purple: Analytical spectrum at different sample rates.
Right: Black: model spectrum, blue: fixed dead time effect, red: transmission function (X 10).

Fixed paralyzable dead time

We have applied the two types of fixed dead time, the non-paralyzable and the paralyzable detector, to the computer generated, randomly sampled velocity signal with a von Karman spectrum (see Eq. (11) later). Figure 4 shows that the spectral bias can be significant when the mean time between samples approaches the dead time, and that the two types of dead time have very different effects on the measured spectrum. The black curve shows the ideal case of zero dead time. The part of the spectrum above the constant noise floor represents the true spectrum. The blue curve shows the resulting spectrum in case of a non-paralyzable detector. The effect of the convolution with the dead time function is clearly visible. The paralyzable detector loses many data due to the increased dead time, and the spectrum shows a loss of power, especially at low frequencies. At high frequencies, the spectral offset reflects the difference in the reduced sampling frequency.

Dead time with an LDA burst processor

The burst type LDA presents a special case of paralyzable dead time. The dead time is the variable residence time plus possibly a small fixed time for transferring the measurement to the data processor.

Looking further into the LDA case, we realize that the dead time problem is identical to the case of two (or more) particles being present within the measurement volume at the same time. It is often assumed that only one particle is present in the MV at any one time, but when we want to measure high frequency turbulence spectra, it is desirable to have a high sample rate in order to obtain a high dynamic range between the true spectrum and the spectral offset. However, this is exactly the condition that can lead to more than one

particle in the measurement volume and thus to dead time effects. We must consider in more detail what occurs in an LDA at high sample rates.

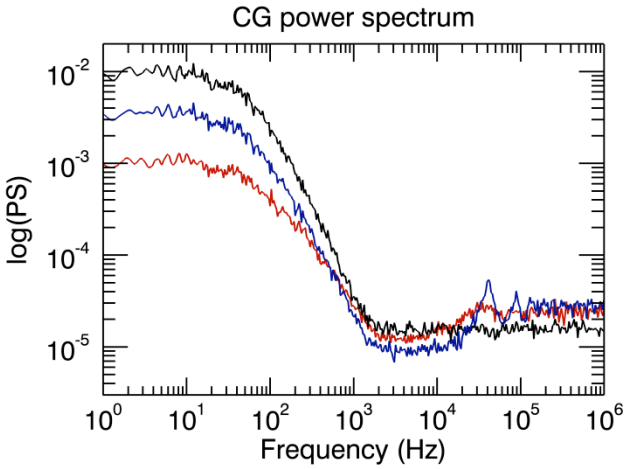

Fig 4. Power spectral bias due to fixed dead time effects. Black: zero dead time, $\nu_0 = 71626$, blue: non-paralyzable detector, $\nu_0 = 25732$, red: paralyzable detector, $\nu_0 = 12986$.

Multiple particles in the MV introduce phase-shifts in the Doppler signal that cannot be distinguished from a fluctuating velocity signal (c.f. George *et al.* 1978, Buchhave *et al.* 1979). In a burst detector, the interference between particles may result in longer or shorter bursts. Figure 5 shows a couple of situations: In the first one, two particles scatter Doppler modulated light bursts that happen to be in phase at the detector. The detector will see this as one sample with an extended residence time. This may be described as a case of a paralyzable detector. The second case is one of two particles, both within the measurement volume, but scattering light that is out of phase at the detector. If the dip in the signal envelope due to the destructive interference is low enough, the system will see this as two particles arriving close to each other. Thus the result of a high particle arrival rate will be a broadening of the distribution of possible residence times and thus a wide range of possible dead times.

Fortunately, it will still be possible to describe the dead time effects since we measure the residence time for each sample, and the dead time distribution will be known. However, this case cannot be described as a simple case of fixed paralyzable or non-paralyzable dead time. Instead, we see the LDA case as an example of detection with a varying dead time, the measured residence time.

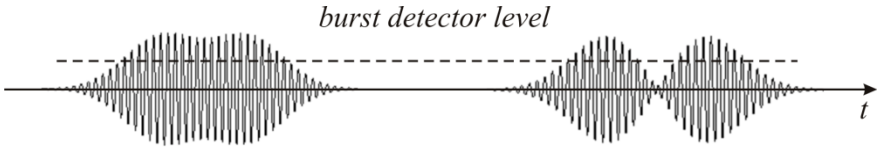

Fig 5. Case of two particles in MV at the same time. Left: scattered Doppler bursts in phase, Right: scattered Doppler bursts out of phase.

4. Analytical description of LDA dead time

The probability density of the measured residence times depends on the flow properties, and we do not have an exact analytical expression. However, we do have the measured residence time data. Figure 6(a) shows the measured residence time probability distribution for our reference spectrum. It turns out that the so-called Weibull function allows a nice fit to the residence time density with just two adjustable parameters (Velte 2009) :

$$P(\Delta t_s) = \frac{k}{\lambda}\left(\frac{\Delta t_s}{\lambda}\right)^{k-1} e^{-(\Delta t_s/\lambda)^k} \tag{8}$$

The best fit to the measured data is $k = 1.875$ and $\lambda = 5.0 \cdot 10^{-6}$.

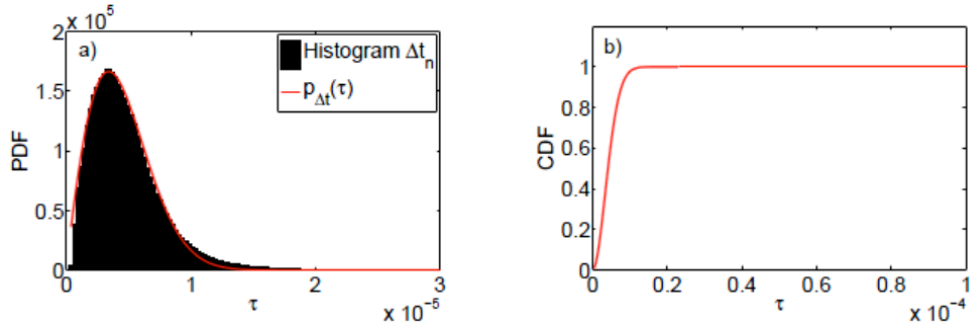

Fig 6. (a) Residence time probability density and matching Weibull density and (b) cumulative Weibull distribution.

This Weibull density is easily integrated to provide the cumulative Weibull distribution function, Figure 6(b):

$$C(\Delta t_s) = 1 - e^{-(\Delta t_s/\lambda)^k} \tag{9}$$

In practice the dead time, Δt_d, and the residence times, Δt_s, are nearly equal so we may consider the Weibull distribution to be a probability distribution describing the probability that a subsequent particle will arrive after the dead time and be registered as an independent measurement. We can use the Weibull density as an expression for a weighted distribution of the non-paralyzable dead time response given in Eq. (3) above. Then the resulting spectrum is simply:

$$S_{0,\Delta t_d,random}(f) = \int_{-\infty}^{\infty} S_{0,\Delta t_s}(f)\, P(\Delta t_s)\, d\Delta t_s \tag{10}$$

The primary effect is that the integral smears out the original dead time window. To investigate the validity of this model, we have used a von Karman turbulent power spectrum with properties matching the measured spectrum:

$$S_{vK}(f) = \frac{1}{62.5} \cdot \frac{1}{\left(1+(f/45)^2\right)^{5/6}} e^{-(f/2500)^{4/3}} \tag{11}$$

We have performed the convolution of the weighted dead time response with the von Karman spectrum with an added constant noise level and arrived at the result shown in Figure 7:

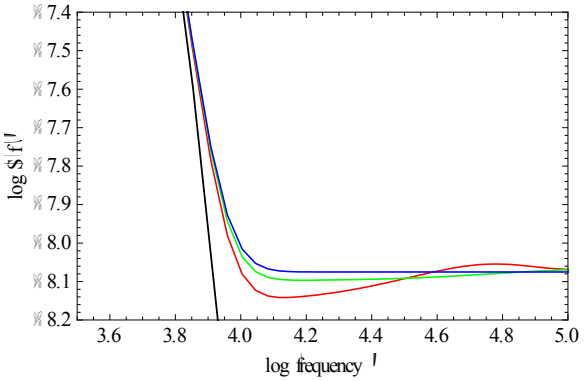

Fig 7. von Karman spectrum convolved with the weighted dead time response. Black: von Karman reference spectrum, Blue: No dead time, Green: Weibull dead time distribution based on measured residence times, Red: Weibull dead time distribution based on measured residence times plus 4 μs fixed dead time.

As we can see, this derivation explains some of the features of the spectrum, but the Weibull density does not in itself sufficiently account for the dip in the spectrum. Thus, the measured residence time density alone does not explain the dip. It appears that the processor does indeed have a finite data transfer time and thus the dead time is not exactly equal to the residence time in the present case. However, a small amount of fixed dead time added to the Weibull distribution does show the expected dip as can be seen in Figure 7.

5. Comparison to measurement

Finally, we process the computer generated (CG) data and the measured velocity data through the same spectral estimator. As the real measurement volume diameter is a quantity that depends on a number of parameters such as particle size, detector/amplifier gain etc. we have adjusted the model measurement diameter d_{MV} to give the best fit to the measured turbulence spectrum. The measurement volume diameter affects the width and location of the dip in the spectrum. Even with this adjustment, the offset level of the computer-generated spectrum is lower than that of the measured spectrum, even with approximately the same data rate. We therefore add random white noise in the frequency domain before converting the frequencies to a time series. Such noise may be detector shot noise, thermal noise in electronics or phase noise in the detected Doppler signal. Addition of this noise raises the constant noise floor. Finally, we add a small amount of fixed dead time ($\approx 4\ \mu$s) to the residence time distribution. This additional dead time could be caused by a small finite processing or data transfer time added to the measured residence time. The two curves, the measured turbulence spectrum and the computer-generated spectrum, now show excellent agreement, see Figure 8: Left hand side shows the spectra with the self-products (the spectral offset) included, right hand side: a constant value subtracted at all frequencies.

Thus, by adjusting measurement volume size, data transmission time and ambient noise we have shown that our model describes the spectral bias introduced by the non-ideal properties of the LDA detector and signal processor.

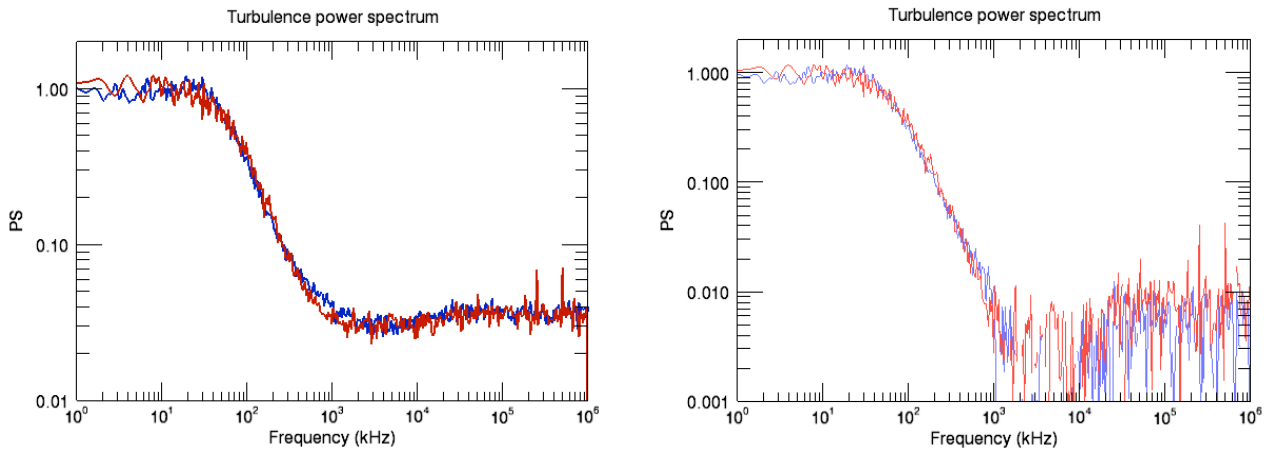

Fig. 8. The measured turbulence spectrum (blue) and the CG spectrum with the measured Weibull residence time distribution plus a small, fixed dead time (red). Left: Self-products included, right: spectral offset subtracted.

6. Conclusion

We have analyzed the effect of processor dead time, either fixed non-paralyzable or fixed paralyzable dead times, acting directly on a model von Karman spectrum. We made an analytical convolution of the dead time function with the von Karman spectrum and we computed the spectrum of a computer generated data series deduced from the same von Karman spectrum. Both methods confirmed the expected effects of the dead time: Reduced spectral power at low frequencies, increased spectral offset at high frequencies and an oscillation starting with a dip in the spectral power at the frequency range corresponding to the measurement volume cut off frequency. We then extended the analysis to describe the laser Doppler anemometer, which introduces a number of additional challenges:

- The residence times, and hence the dead times, are not constant, but have a wide distribution; this can be fitted to a Weibull distribution.
- Due to the way the burst detector is constructed, interpreting bursts that may have any combination of constructive and destructive interference is not straightforward, but requires a more sophisticated dead time model. This model is described above.
- The burst processor appears to require a finite time for data transfer in addition to the residence time.

Despite these issues, we were able to construct a relatively simple, but realistic model for the LDA sampling process, which accurately describes the LDA burst processor.

It is clear that it is advisable, if possible, to reduce the measurement volume size compared to the flow scales, since the dip in the power spectrum is directly related to the probe volume cut-off frequency. In addition, a small measurement volume reduces the loss of data rate due to dead time effects and allows a high average particle concentration, which reduces the spectral offset thereby increasing the dynamic range for the measured spectrum. Further, it is advisable to use fast processing/data transfer to reduce the effect of additional fixed dead time, which contributes to the unwanted oscillation in the spectrum at high frequencies.

7. References

Buchhave P, George WK and Lumley JL (1979) The measurement of turbulence with the laser-Doppler anemometer. Ann Rev Fluid Mech 11:443-504.

Buchhave P, Velte CM and George WK (2014) The effect of dead time on randomly sampled power

spectral estimates. Exp in Fluids 55: 1680.

George WK, Beuther PD and Lumley JL (1978), Processing of random signals. Proceedings of the Dynamic Flow conference, Skovlunde, Denmark, pp757–800.

Gaster M and Roberts JB (1975) Spectral analysis of randomly sampled signals. J Inst Maths Applics 15:195-216.

Gaster M and Roberts JB (1977) The spectral analysis of randomly sampled records by a direct transform. Proc. R. Soc. A, 354:27-58, 1977.

Gaster M (2013) Private Communication.

Velte CM, George WK and Buchhave P (2014) Estimation of burst-mode LDA power spectra. Exp in Fluids 55:1674.

Velte CM Characterization of vortex generator induced flow. PhD dissertation, Technical University of Denmark, 2009.

Zhang W, Jahoda K, Swank JH, Morgan EH and Giles AB (1995) Dead-time modifications to fast Fourier transform power spectra. Astroph J 449:930–935.

http://ltces.dem.ist.utl.pt/lxlaser/lxlaser2014/paper_submission.asp